Landslide Susceptibility Analysis of Shiv-Khola Watershed, Darjiling: A Remote Sensing & GIS Based Analytical Hierarchy Process (AHP)

Article *in* Journal of the Indian Society of Remote Sensing · September 2011

DOI: 10.1007/s12524-011-0160-9

2 authors:

Sujit Mandal
Diamond Harbour Women's University

Ramkrishna Maiti
Vidyasagar University

J Indian Soc Remote Sens (September 2012) 40(3):483–496
DOI 10.1007/s12524-011-0160-9

RESEARCH ARTICLE

Landslide Susceptibility Analysis of Shiv-Khola Watershed, Darjiling: A Remote Sensing & GIS Based Analytical Hierarchy Process (AHP)

Sujit Mondal · Ramkrishna Maiti

Received: 12 April 2011 / Accepted: 31 August 2011 / Published online: 18 October 2011

Abstract In the present study, Remote Sensing Technique and GIS tools were used to prepare landslide susceptibility map of Shiv-khola watershed, one of the landslide prone part of Darjiling Himalaya, based on 9 landslide inducing parameters like lithology, slope gradient, slope aspect, slope curvature, drainage density, upslope contributing area, land use and land cover, road contributing area and settlement density applying Analytical Hierarchy Approach (AHA). In this approach, quantification of the factors was executed on priority basis by pair-wise comparison of the factors. Couple comparing matrix of the factors were being made with reasonable consistency for understanding relative dominance of the factors as well as for assigning weighted mean/ prioritized factor rating value for each landslide triggering factors through arithmetic mean method using MATLAB Software. The factor maps/thematic data layers were generated with the help of SOI Topo-sheet, LIIS-III Satellite Image (IRS P6/Sensor-LISS-III, Path-107, Row-052, date-18/03/2010) by using Erdas Imagine 8.5, PCI Geomatica, Arc View and ARC GIS Software. Landslide frequency (%) for each class of all the thematic data layers was calculated to assign the class weight value/rank value. Then, weighted linear combination (WLC) model was implied to determine the landslide susceptibility coefficient value (LSCV or 'M') integrating factors weight and assigned class weight on GIS platform. Greater the value of M, higher is the propensity of landslide susceptibility over the space. Then Shivkhola watershed was classified into seven landslide susceptibility zones and the result was verified by ground truth assessment of existing landslide location where the classification accuracy was 92.86 and overall Kappa statistics was 0.8919.

Keywords Remote sensing & GIS · Analytical Hierarchy Process (AHA) · Landslide Susceptibility · Frequency Ratio (FR)

S. Mondal (✉)
Department of Geography,
Raja N.L.Khan Women's College,
Paschim Medinipur, West Bengal 721102, India
e-mail: mandalsujit2009@gmail.com

R. Maiti
Department of Geography and Environment Management,
Vidyasagar University,
Paschim Medinipur, West Bengal 721102, India
e-mail: ramkrishnamaiti@yahoo.co.in

Introduction

Several attempts to reduce landslide risk were made through studying the history of management of landslide terrain by constructing protective structures or monitoring and warning systems, or through the ever-increasing sophisticated methods for mapping and delineating areas prone to landslides (Dai and

Lee 2002). Landslides were the result of two interacting sets of forces; '*the precondition factors',* naturally induced which govern the stability conditions of slopes, and '*the preparatory and triggering factors',* induced either by natural factors or by human intervention. These triggers are intensive, geologically speaking short-term processes that irreversibly change the slope and cause the landslide. Landslide analysis was mainly done by assessing susceptibility as well as hazard and risk (Einstein 1988). Sharma (2006) introduced an emerging geotechnical approach for landslide hazard zonation. GIS based landslide hazard zonation approach was applied by Carrara et al. (1995); Saha et al. (2002); and Caiyan and Jianping (2009). Jibson et al. (2000); Luzi et al. (2000); Parise and Jibson (2000); Rautelal and Lakheraza (2000); Donati and Turrini (2002); and Zhou et al. (2002) applied the probabilistic model for landslide risk and hazard analysis. An integrated approach for landslide susceptibility mapping using Remote Sensing and GIS was presented by Sarkar and Kanungo (2004); Sharifikia (2007) Pandey et al. (2008); and Nithya and Prasanna (2010). A number of predictive as well as probabilistic models were used for identifying areas of landslide risk by Gokceoglu et al. (2000); Pistocchi et al. (2002); Lee, Choi and Min (2004); Barbieri & Cambuli (2009) and Bathurst et al. (2010). The Landslide hazard risk and susceptibility in the mountainous region was studied using various model by Varnes (1984), Lee and Choi (2003), Lee and Ryu (2004), Van Westen et al. (2008), Vijith and Madhu (2008) and Kouli et al. (2010). Atkinson and Massari (1998) applied a generalized linear model for analyzing landslide susceptibility. Probabilistic slope failure modes as well as logistic regression models were used for analyzing risk from slope instability by Rowbotham and Dudycha (1998), Lee and Pradhan (2006), Muthu and Petrou (2007), Pradhan (2010), Pradhan and Lee (2010a). Neural network model for susceptibility analysis was performed by Pradhan and Lee (2010b), Pradhan and Lee (2010c). *Analytical Hierarchy Approach* (AHA), a semi-quantitative method based on decomposition, comparative judgment, and synthesis of priorities for regional susceptibility studies, was introduced by Saaty (1980), and subsequently applied and elaborated by Soeters and Van Westen (1996); Guzzetti et al. (1999); Malczewski (1999); Barredo et al. (2000); Mwasi (2001); Nie et al. (2001) and Yagi (2003). In the present study, *Analytical Hierarchy Approach* (AHA) was applied to prepare landslide susceptibility map of the Shivkhola Watershed for its specialty of couple comparing of landslide factors and evaluating pair-wise rating inconsistency.

The Study Area

The study area shiv-khola watershed (Fig. 1) of Kurseong division in Darjiling district is one of the vulnerable zones because of frequent occurrence of slope failure every year, during monsoon period. It is situated between Kurseong town to the north and Tindharia to the south extending 88°17′ 30″ E to 88° 23′45″ E and 26°50′15″ N to 26°53′35″ N. The present works have attempted for the identification of the spatial distribution of potential slope instability in a representative drainage basin, over which the attributes of land, soil and water exhibit a spatial order away from the water divide in an interacting combination with human actions.

Materials and Methods

All the thematic data layers of landslide inducing factors were made using ERDAS Imagine 8.5, Arc View and ARC GIS Software. In the present work, Analytical Hierarchy Process (AHP) was applied and a weighted linear combination (WLC) was performed by integrating factors weight and class weight/rank value to extract the landslide susceptibility coefficient value (M) for each pixel in the Shivkhola watershed. The data used in the present study are satellite image (IRS P6/Sensor-LISS-III, Path-107, Row-052, date-18/03/2000) and modified SRTM data with scene size 1° latitude and 1° longitude (Date-5th April, 2008) and Google Earth Image (1st Sept. 2010), Geological Map (Geological Survey of India, East Kolkata), and Topographical map (Survey of India; 78B/5). The topographical map and satellite image were used as base maps of the study area for field data identification and collection. The entire methodology to achieve the goal could be summarized under the following heads.

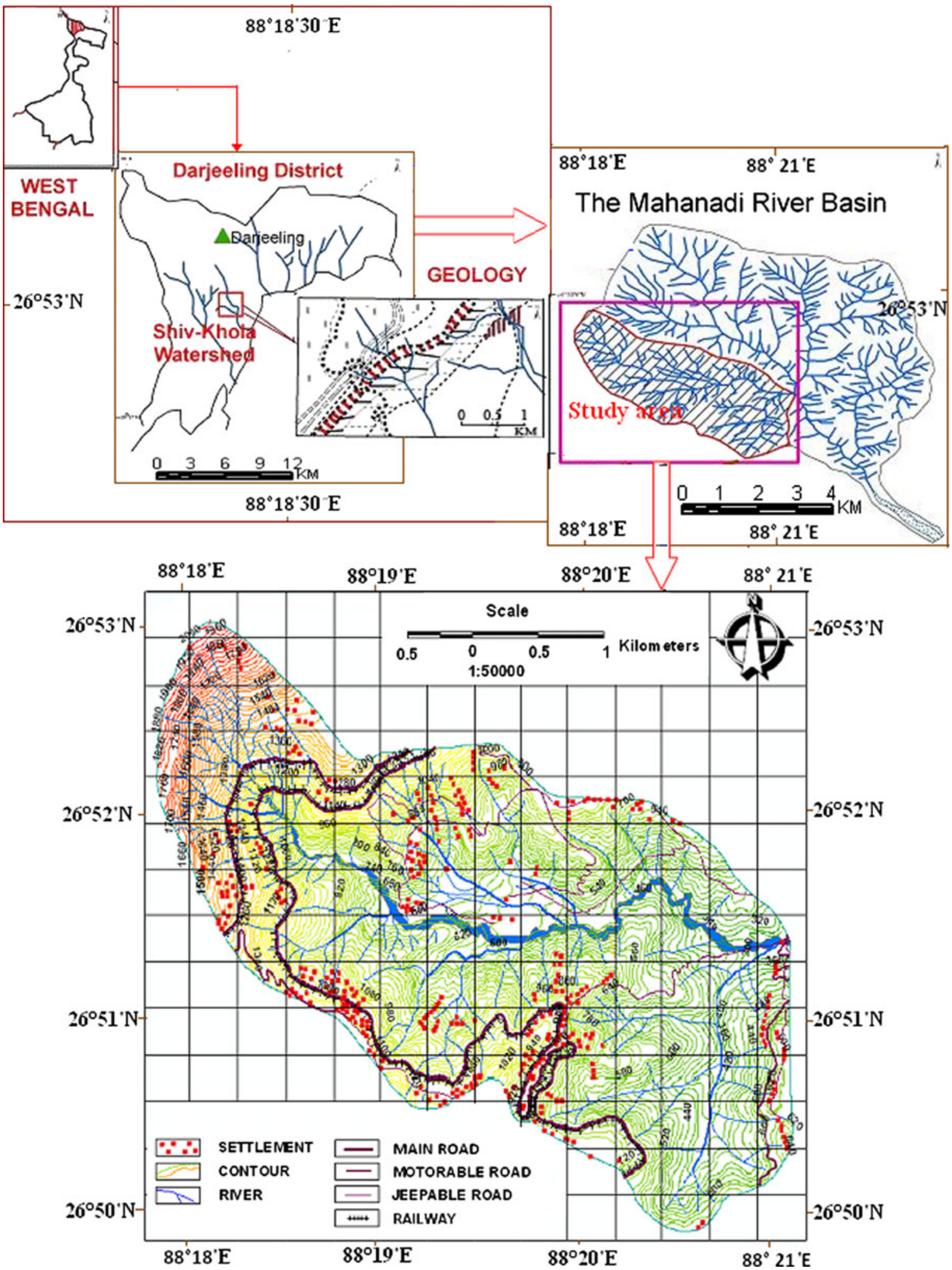

Fig. 1 Location map of the Shiv-khola watershed

Determination of Landslide Causative Factors Map

The common method to study the landslide causative factors was to use questionnaire (oral judgement) and empirical study of the landslides inside the watershed associated to intensive field works. After thorough investigation of the field, nine landslide causative factors such as lithology, slope angle, slope aspect, slope curvature, drainage, upslope contributing area (U.C.A.), land use/land cover, road contributing area (RCA) and settlement density (anthropogenic) were taken into account to produce landslide susceptibility map of the Shivkhola watershed and finally their hierarchical arrangement were made on priority basis. In Shivkhola watershed, a hilly basin, the triggering factors such as rainfall and earthquake were difficult to gauge due to extreme spatial variation and could not be considered here due to non-availability of past records and their relation with landslide phenomena.

Preparation of Landslide Inducing Factors Maps

Firstly, the *contour map* at 20 m interval was prepared and digitized from the SOI topographical map (1987) at the scale of 1: 50000 and subsequently employed for generating the DEM using the ARC GIS Software. *Slope gradient*, *slope curvature* and *slope aspect maps* were extracted from DEM with 25-m grid cell size and classification was made following the earlier works of Anbalagan (1992) and Dhakal et al. (2000). Slope gradient map was classified into 10 classes considering the steepness of the terrain. Slope Curvature was classified into 9 classes as per convexity and concavity of the mountain slope. Slope Aspect maps was made and classified into 9 following the direction of slope facets. The *lithological map* of the concerned study area was collected from Geological Survey of India (GSI), Kolkata (Eastern Region) and necessary modifications were incorporated after field investigation. Final lithological map was prepared with seven rock types and transformed into raster value domain on ARC GIS platform. Class Weight value for each lithological class was assigned according to rock mass strength, described by GSI. Drainage density map (the length of drainage in km/sq.km) was made on the grid resolution of 23.5×23.5 m from the topographic map and classified with six equal intervals. *Upslope Contributing Area* is an effective indicator of drainage concentration over space. The place having more contributing area encompasses more soil saturation and reduces soil cohesion. The specific contributing area (total contributing area divided by the contour length) was computed by distributing flow from a pixel among its entire lower elevation neighbor pixel (Borga et.al. 1998). Quinn et al. (1991) proposed that the Fraction of Flow (F_i) allocated to each lower neighbour (i) is to be determined by Eq. 1.

$$Fi = \frac{\text{SiLi}}{\sum \text{SiLi}} \tag{1}$$

Where the summation is for the entire lower neighbor;

S is the directional slope, and
L is an effective contour length that acts as the weighting factor.

The value of L used here is 10 m of the pixel size of the cardinal neighbour and 14.14 m of the pixel diagonal for diagonal neighbour.

An upslope contributing area map was prepared based on calculated contributing area for each grid (0.25 sq.km) and considering the highest (21.05 sq.km.) and lowest value (0.5 sq.km.) it was divided into 6 equal classes. Construction of roads and expansion of human settlement in the area were the major human intervention. Road Contributing Area (RCA) map was prepared with eight equal classes estimating road contributing length (RCL) and road contributing width (RCW) for each 0.25 sq.km grid from the concerned SOI Topo-sheet and then it was transformed into raster value domain on ARC GIS Platform. Settlement density map was made by applying 3*3 karnel on ARC GIS Platform and the watershed was classified into seven equal density classes.

Identification of Major Landslide Location and Determination of Landslide Frequency (%)

Most of landslides observed in the study area were debris slides. In some places rotational and complex type of landslide phenomena were observed during the field investigation. Most of the landslide in the Shivkhola Watershed covers an area extent of 600 m^2 to 2300 m^2. High resolution satellite image such as SPOT PAN of 10-m resolution and ATM imagery of 7.5-m resolution were applied by Mason et al. (1998) for landslide detection. In this study, intensive field investigation was made with GPS to identify major landslide

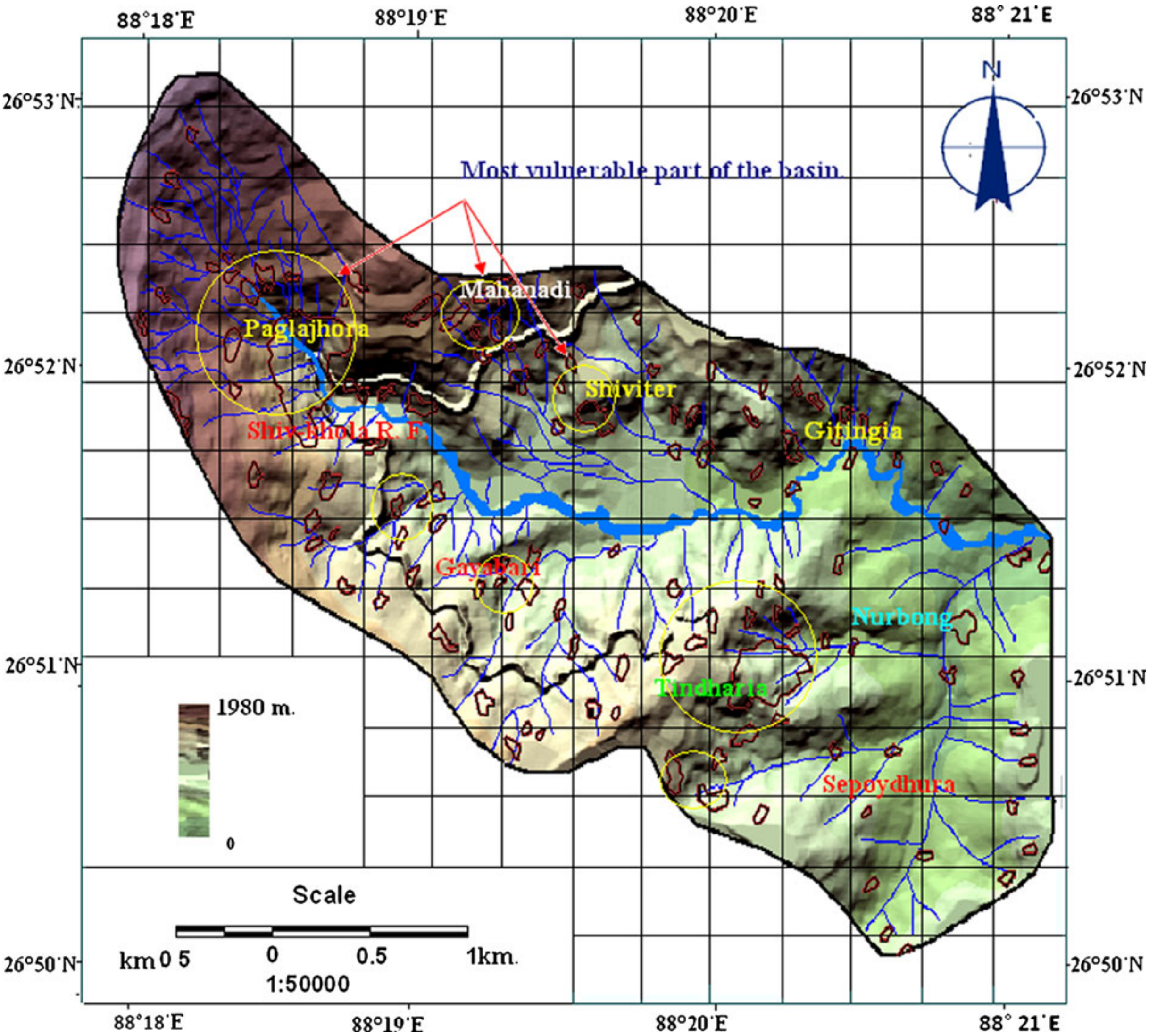

Fig. 2 Landslide distribution map

locations, intensive surveys were conducted with Clinometer, Abney's Level and Dumpy level. LISS III images (2000), SRTM data (2008) and Google Earth Image (2010) were linked with the surveyed landslide by thorough rectification. Mapped landslides were cross-checked by field verification and the map was modified accordingly. Special care was taken for shadow slopes to avoid major errors. Then, it was digitized and converted into raster value domain through ARC GIS Software. But in calculating *landslide frequency (%)* for each range/class of the concerned factors, only major landslide location points were considered that is cited in the Eq. 2. Ranking values/class weight values for each class were assigned on the basis of derived landslide frequency (%) (Ahmadi 2003) (Fig. 2).

$$\textit{Landslide frequency}\ (\%) = (f_2 \div f_1) \times 100 \qquad (2)$$

f_2 number of major landslide location in each class.
f_1 total number of major landslide location.

Table 1 Preference scale between two parameters in AHP (Saaty 2000)

Degree of Preferences	Numerical Scales	Explanation
1. Extremely	9	The evidence of favoring one activity over another is of the highest degree possible of an affirmation.
2. Very strongly	7	An activity is strongly favored over another and its dominance is showed in practice.
3. Strongly	5	Experience and judgement strongly or essentially favor one activity over another
4. Moderately	3	Experience and judgement slightly to moderately favor one activity over another
5. Equally	1	Two activities contribute equally to the objective.
6. Intermediate values	2,4,6,8	Used to represent compromises between the preferences in weights 1,3,5,7 and 9
7. Opposite	Reciprocals.	Used for inverse comparison

Analytical Hierarchy Process (AHP) and Landslide Susceptibility Map

Analytical Hierarchy Process (AHP) is a semi-quantitative method, which includes a pair -wise comparison of various landslide triggering factors to determine prioritized factors weight. Factors weight for all thematic maps were estimated by developing a pair-wise comparison matrix as described by Saaty (1990, 1994), and Saaty and Vargas (2001).

Preference of Each Factor and its Conversion into Numerical Values

In the Analytical Hierarchy Process (AHP) different factors preference and their conversion into numerical value were being accomplished developing consistent couple comparing matrix. In this method, the preference of a factor as compared with the other factor was taken into account to get the factors weight, and for this, a pair wise comparison matrix with numerical values was developed in Table 1.

Couple/Pair Comparing of the Entire Landslide Inducing Factors, Prioritized Rating Value (Eigenvectors) and Consistency Ratio

To construct couple comparing matrix of all the individual factors, each factor was rated against every other factor by assigning a relative dominant value ranging between 1 and 9. The value also varies between the reciprocals ½ and 1/9 for inverse comparison. Then, arithmetic mean method was used to calculate each alternative prioritized factor rating value/eigenvalue of all landslide triggering factors by using MATLAB Software.

Another appealing feature of the AHP is the ability to evaluate pair-wise rating inconsistency. The eigenvalues enable to quantify a consistency measure which is an indicator of the inconsistencies or intransivities in a set of pair-wise ratings. Saaty (2000) presented that for a consistent reciprocal matrix, the largest eigenvalue, λ_{Max} , is equal to the number of comparisons n.

In AHP, an index of consistency, known as the CR (consistency Ratio), is used to indicate the probability that the matrix judgements were randomly generated (Saaty 1977).

$$\text{Consistency Ration (CR)} = \frac{\text{CI}}{\text{RI}} \tag{3}$$

Where RI is the average of the resulting consistency index depending on the order of the matrix given by Saaty and CI is the consistency index that is expressed in the following equation.

A measure of consistency, called consistency index CI, is defined as follows:

Table 2 Random index (RI)

N	1	2	3	4	5	6	7	8	9	10	11	12	13	14	15
RI	0	0	.58	.90	1.12	1.24	1.32	1.41	1.45	1.49	1.51	1.53	1.56	1.57	1.59

Table 3 Calculation of prioritized factors weight

	1	2	3	4	5	6	7	8	9	PFW*
Lithology	1	3	4	5	7	6	8	9	2	0.300
Drainage	1/3	1	2	3	5	4	6	7	1/2	0.149
Slope gradient	1/4	1/2	1	2	3	4	6	7	1/3	0.110
Slope Aspect	1/5	1/3	1/2	1	3	2	5	7	1/5	0.080
Slope Curvature	1/7	1/5	1/3	1/3	1	2	3	4	1/7	0.047
U.C.A.	1/6	1/4	1/4	1/2	1/2	1	1/2	3	1/6	0.034
Land use/ land cover	1/8	1/6	1/6	1/5	1/3	2	1	1/2	1/8	0.027
R.C.A.*	1/9	1/7	1/7	1/7	1/4	1/3	2	1	1/9	0.022
Settlement Density	1/2	2	3	5	7	6	8	9	1	0.231

*RCA-Road Contributing Area and *PFW-Prioritized Factor Weight

$$\text{Consistency Index(CI)} = \frac{\lambda_{\max} - \text{n}}{n-1} \quad (4)$$

Saaty (2000) randomly produced reciprocal matrices using scales 1/9, 1/8, 1/7,……,1……8, 9 to evaluate a so called random consistency index (RI). The average RI of 500 matrices is given in the following table (Table 2).

According to Saaty, if the value of the CR is smaller or equal to 10%, the inconsistency is acceptable, but if the CR is greater than 10%, the subjective value judgement needs to be revised (Saaty 1977). In the present work, a couple comparing matrix was constructed to arrange landslide triggering factors hierarchically on the basis of prioritized factor rating value/eigenvector with reasonable consistency (Table 3).

Value Assignment/Quantification to Each Classes of the Factors Map

Quantification of the factors and weighting their classes are done with regard to landslides frequency (%) in the homogeneous units that are similar in the entire factors view point, but one of the factors is variable in its classes (Nagarajan et al. 2000). By using remote sensing and GIS, all the prepared thematic maps were quantified and rasterised to specific pixel size. A binary method was used for cross matching of each thematic map with respect to the landslide distribution map. Analyzing the landslide frequency (%) of each class of all the triggering factors all classes was valued from 0 to 100 (Ahmadi 2003). The class of each factor which had the maximum landslide contributing units containing the maximum value 100 and proportional with that all classes of individual factor were given different scores (Table 4). A numerical scale was devised to assign the scores for each class which range from 1 to 10 and all the factors map were reclassified using spatial analyst tools on ARCGIS platform. The value ‘1’ was assigned to lowest landslide contributing units whereas the highest landslide contributing unit was assigned as the value of ‘10’.

Application of Model and Landslide Susceptibility Map

In the AHP, landslide susceptibility co-efficient (LSC)/landslide susceptibility index (LSI) was derived using weighted linear combination model for each pixel by summation of each factor’s weight (W_i) multiplied by class weight/ rating (R_i) of each referred landslide triggering factor, which is ascribed in the following equation.

$$LSC(M) = \sum\nolimits_{i=1}^{n} (W_i \times R_i) \quad (5)$$

The Shiv-khola Watershed was classified into 6 landslide susceptibility zones i.e. 1. Very high, 2. High, 3. Moderately high, 4. Moderate, 5. Low and 6. Very low. The ‘M’ value varies from ‘0.28’ to ‘6.87’. To classify the watershed, landslide susceptibility coefficient frequency diagram was studied and abrupt change points (landslide threshold boundaries) i.e. 0.92, 1.85, 2.70, 3.95, and 5.25 were taken into account and by ‘slicing’ operation landslide susceptibility map was made. A 3×3 ‘majority filter’ was applied to the map as a post-classification filter to reduce the high frequency variation. Higher the value of ‘M’, greater was the propensity of landslide phenomena and vice versa. To assess the probability

Table 4 Landslide frequency (%) and assigned ranking value/class weight/score

Factors	Factor weight (w)	Categories		Landslide frequency (%)	Ranking/score
Slope	0.149	0–7.17	1	5.67	1
		7.17–14.34	2	6.24	2
		14.34–19.92	3	5.88	3
		19.92–24.97	4	8.22	4
		24.97–29.75	5	8.74	5
		29.75–34.53	6	11.85	6
		34.53–39.57	7	10.71	7
		39.57–45.95	8	12.73	8
		45.95–54.71	9	14.70	9
		54.71–67.73	10	17.94	10
Slope Aspect	0.110	Flat	1	3.06	0
		North	2	17.14	8
		North East	3	11.67	4
		East	4	15.53	6
		South East	5	12.54	7
		South	6	13.10	5
		South West	7	1.05	2
		West	8	2.40	1
		North West	9	2.32	3
Curvature	0.080	−25.87–11.41	1	22.21	6
		−11.41–−5.73	2	26.75	5
		−5.73–−2.33	3	23.02	4
		−2.33–−0.63	4	15.39	3
		−0.63–0.50	5	3.84	2
		0.50–2.49	6	4.25	2
		2.49–7.31	7	8.53	3
		7.31–14.69	8	14.21	4
		14.69–24.33	9	24.80	5
Drainage Density	0.047	0–1.90	1	1.61	1
		1.90–3.80	2	1.99	2
		3.80–5.71	3	4.80	3
		5.71–7.61	4	2.71	4
		7.61–9.51	5	4.57	5
		9.51–11.41	6	16.67	6
		11.41–13.31	7	28.48	7
		13.31–15.21	8	24.28	8
		15.21–17.12	9	35.37	9
		17.12–19.02	10	35.86	10
Upslope Contributing Area	0.034	<5.00	1	76.56	3
		5.00–10.00	2	66.67	1
		10.00–15.00	3	100	5
		15.00–20.00	4	100	5
		>20.00	5	100	5
Lithological Composition	0.300	Darjiling gneiss	1	73.07	7

Table 4 (continued)

Factors	Factor weight (w)	Categories		Landslide frequency (%)	Ranking/score
		Chungtung formation	2	56.25	9
		Lingtse granite	3	61.54	8
		Gorubathan formation	4	69.23	8
		Reyang formation	5	65.52	6
		Damuda formation(Gondwana)	6	43.75	5
		Siwalik groups	7	55.56	4
Land use/land cover (LULC)	0.027	Tea	1	12.55	7
		Jungle	2	11.74	4
		Open forest	3	3.57	5
		Degraded forest	4	7.36	6
		Dense forest	5	9.18	3
		Bared surface	6	7.96	5
		Mixed forest	7	20.11	4
		Agricultural land	8	11.59	2
		Settlement	9	8.23	7
		Roads	10	10.05	8
Road Contributing Area (RCA)	0.022	<0.002	1	4.35	1
		0.002–0.004	2	5.79	2
		0.004–0.006	3	5.25	3
		0.006–0.008	4	10.28	4
		0.008–0.010	5	17.57	5
		0.010–0.012	6	19.27	6
		0.012–0.014	7	22.05	7
		>0.014	8	15.44	5
Settlement Density	0.231	Very low	1	5.25	1
		Low	2	10.24	2
		Moderately low	3	11.54	3
		Moderate	4	15.38	5
		Moderately high	5	14.53	4
		High	6	17.28	6
		Very high	7	25.78	7

of landslide susceptibility and also to indicate the chances of landslide occurrence in each zone Frequency Ratio (FR) was calculated by means of a ratio between landslide frequency (%) and landslide susceptibility area (%).

Verification of Landslide Susceptibility with Field Data/Accuracy Assessment

The accuracy assessment of the landslide susceptibility map was made by using Erdas Imagine (8.5). Accuracy assessment is a general term for comparing the classification with geographical data that are assumed to be true, in order to determine the classification process. Basically, the true data were derived for ground truth verification with the help of GPS from the existing/active 28 landslide location. Simultaneously, a set of randomly selected 28 reference pixels points from the classified image corresponding to the true data were used for evaluating the validity of landslide susceptibility map (Congalton 1991).

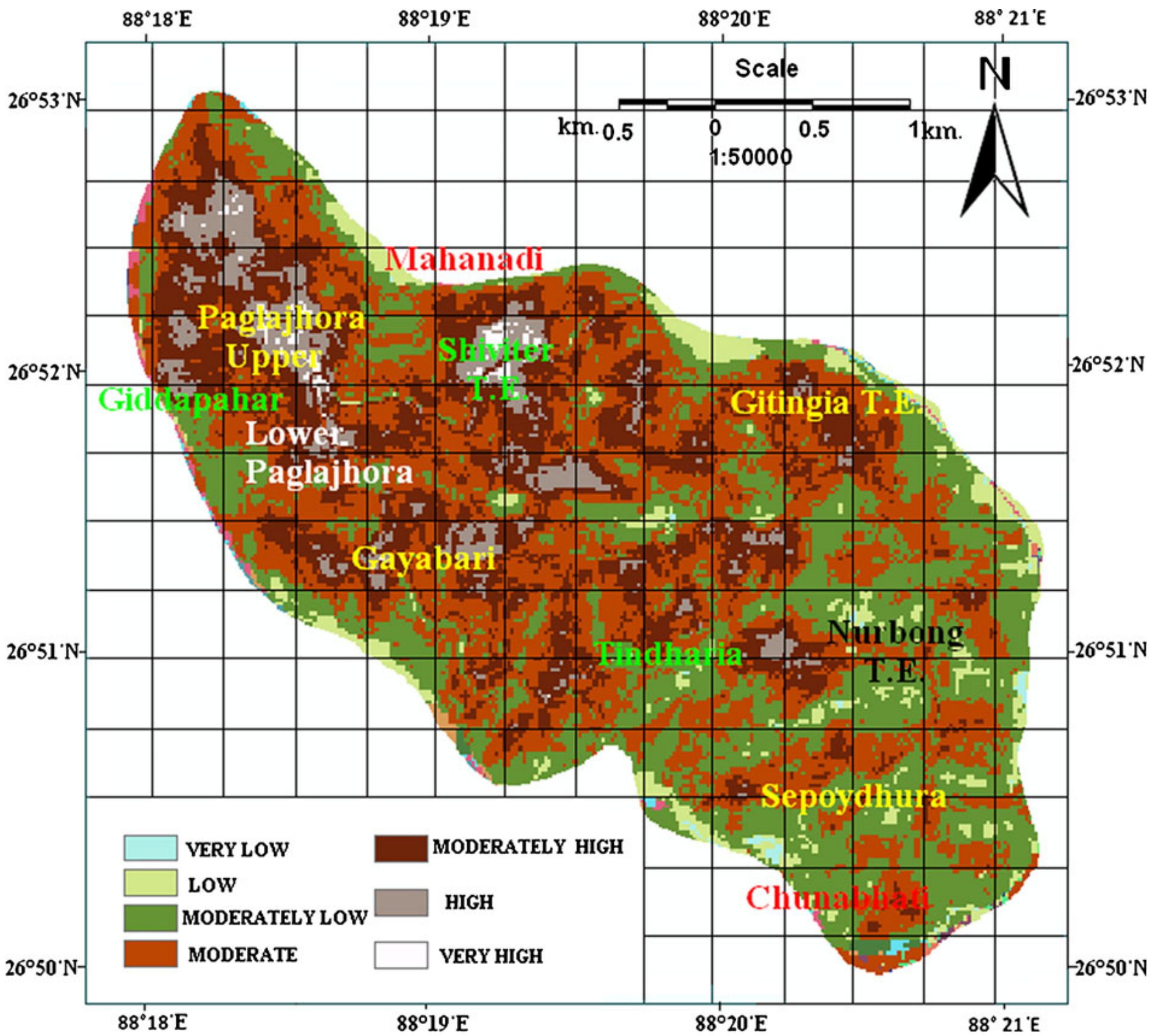

Fig. 3 Landslide susceptibility map

Table 5 Areal distribution of Landslide susceptibility (%), landslide affected area (%) and Frequency ratio (FR)

Susceptibility classes	Area (pixels)	% of area	Number of landslide points	Frequency ratio (FR)
Very low (VL)	125	0.45	0 (0%)	0.00
Low (L)	1828	6.51	1 (2%)	0.30
Moderately low (ML)	8402	29.93	4 (8%)	0.27
Moderate (M)	9951	35.45	9 (18%)	0.51
Moderately high (MH)	5997	21.37	15 (30%)	1.40
High (H)	1604	5.71	12 (24%)	4.20
Very high (VH)	746	2.66	6 (12%)	4.51

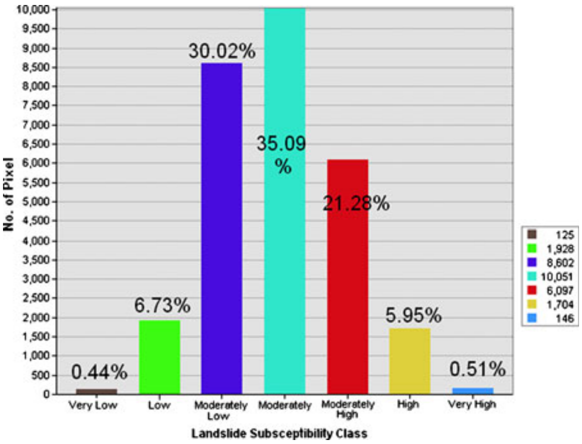

Fig. 4 Pixel wise landslide susceptibility distribution

Results and Discussion

The study concluded that Lower Paglajhora, Shiviter and Tindharia were very highly susceptible to landslide; Upper Paglajhora, Gayabari, 14 Miles Bustee and Nurbong T.E. were characterized by high landslide susceptibility; Mahanadi and Giddapahar were of moderate landslide potentiality; and marginal waxing slope of water divide and low-central waning slope were registered with low landslide susceptibility (Fig. 3).

The study revealed that more than 60% area of the Shivkhola watershed was classified as being in the moderate to very high landslide susceptibility with 75% landslide phenomena. Moderately low, low and very low susceptibility zones together accommodate 10% of the landslide phenomena (Table 5) and 37.16% of the total area (Fig. 4). To evaluate the validity of the results, the probability of landslide in each susceptibility class was derived by means of ratio between landslide frequency (%) and the area coverage of landslide susceptibility (%) for each and individual classes. The value ranges from 0 to 4.51. The value '0' indicates lower the chances of landslide occurrence within the watershed. Ratio value of '1' considered the area having the equal chance of landslide occurrence in the area. The calculated ratio value of 4.51 and 4.20 for very high and high landslide susceptibility zones of the watershed depicts the higher probability of having landslide activities compared to zones having less than ratio value of '1' (VL, L, ML, and M). Here, frequency study shows that more than 8% area is experienced with high landslide probability, around 50% with moderate landslide probability and remaining area with low landslide probability.

The comparison between assumed true data and randomly selected data from the classified image shows that the overall classification accuracy is 92.86% and overall Kappa Statistics is 0.8919%. The class wise accuracy result is shown in Table 6.

Conclusion

Pre-slide management of slope seems to be more important for prevention of landslides which requires identification of the susceptible zones. The present work identifies vulnerable zones of varied priority applying systematic approach of slope evolution where the stability is expressed as a functional combination of numbers of factors. The analysis of prepared *Landslide Susceptibility*

Table 6 Accuracy assessment/comparison of landslide susceptibility with field data

Class name	Classified total	Number correct	Producers correct	Users accuracy	Accuracy total
Very low	0.00	1	0	–	–
Low	0.00	0	0	–	–
Moderately low	0.00	0	0	–	–
Moderate	12	11	11	91.67%	100.00%
Moderately high	2	2	2	100.00%	100.00%
High	11	11	10	90.91%	90.91%
Very high	3	3	3	100.00%	100.00%
Total =	28	28	26		
Overall classification Accuracy = 92.86%					
Overall Kappa Statistics = 0.8919					

Map reveals that the scarp at middle portion of watershed was highly prone to slope instability because of the existence of the slip surface below the upper rock bed, more upslope contributing area, saturation excess surface run-off, steep slope and dominant human intervention along NH-55 through plying of heavy vehicles and concentration of settlement for harnessing accessibility. The estimated prioritized factor rating values for slope gradient, slope aspect, slope curvature, lithology, drainage, land use/land cover, upslope contributing area (UCA), road contributing area (RCA) and settlement density are 0.11, 0.08, 0.047, 0.300, 0.149, 0.027, 0.034, 0.022 and 0.231 respectively which has depicted lithology, expansion of settlement, and slope are three dominant contributing factors to slope failure in the Shivkhola Watershed. The present work suggests that rational management of potential slope failure zones, where the danger is not exposed yet, is of most importance and to be considered as equally important to that of immediate response to a fresh landslide. To check and prevent landslide phenomena in the Shiv-khola watershed, site-specific management of slope is necessary which may include armouring the drain along the junction between road and the hill slope, introducing jhora training and geo-textile method, constructing retaining wall, breast wall and catch water drain, monitoring of sub-surface water, introduction of fern vegetation, strict and continuous monitoring along NH-55, and road diversion to avoid the Paglajhora-Sinking Zone.

References

Anbalagan, R. (1992). Landslide Hazard Evaluation and Zonation mapping in mountainous terrain. *Engineering Geology, 32*, 269–277.

Atkinson, P. M., & Massari, R. (1998). Generalized linear modeling of susceptibility to landsliding in the central Apennines, Italy. *Computer & Geosciences, 24*, 373–385.

Barbieri, G., & Cambuli, P. (2009). The weight of evidence statistical method in landslide susceptibility mapping of the Rio Pardu Valley (Sardinia, Italy), 18th World IMACS/MODSIM Congress, Cairns, Australia, 13–17.

Barredo, J. I., Benavidesz, A., & Van Westen (2000). Comparing heuristic landslide hazard assessment techniques using GIS in the Tirajana basin, Gran Canaria Island, Spain. *JAG, 2*, 9–23.

Bathurst, J. C., Bovolo, I. C., & Cisneros, I. F. (2010). Modelling the effect of forest cover on shallow landslides at the river basin scale. *Ecological Engineering, 36*, 317–327.

Borga, M., Dalla Fontana, G., Da Ros, D., & Marchi, L. (1998). Shallow landslide hazard assessment using a physically based model and digital elevation data. *Environmental Geology 35*(2–3), 81–88.

Caiyan, W. U., & Jianping, Q. (2009). Relationship between landslides and lithology in the Three Gorges Reservoir area based on GIS AND Information Value Model. *Higher Education Press and Springer-Verlag, 4*, 165–170.

Carrara, A., Cardinali, M., Guzzetti, F., & Reichenbach, P. (1995). *GIS-Based techniques for mapping landslide hazard in Geographical Information System in Assessing Natural Hazards*. Dordrecht: Academic.

Congalton, R. (1991). A review of assessing the accuracy of classification of remotelysensed data. *Remote Sensing of Environment, 37*, 35–46.

Dai, F. C., & Lee, C. F. (2002). Landslide characteristics and slope instability modeling using GIS; Lantau Island, Hong Kong. *Geomorphology, 42*, 213–228.

Dhakal, A. S., Amada, T., & Aniya, M. (2000). Landslide hazard mapping and its evaluation using GIS: An investigation of sampling schemes for a grid-cell based quantitative method. *Photogrametric Engineering and Remote Sensing, 66*(8), 981–989.

Donati, L., & Turrini, M. C. (2002). An objective and method to rank the importance of the factors predisposing to landslides with the GIS methodology, application to an area of the Apennines (Valnerina; Perugia, Italy). *Engineering Geology, 63*, 277–289.

Einstein, H. H. (1988). Landslide risk assessment procedure. Proceedings of the Fifth International Symposium on Landslides. pp. 1075–1090.

Gokceoglu, C., Sonmez, H., & Ercanoglu, M. (2000). Discontinuity controlled probabilistic slope failure risk map of the Altindag (Settlement) region in Turkey. *Engineering Geology, 55*, 277–296.

Guzzetti, F., Carrara, A., Cardinali, M., & Reichenbach, P. (1999). Landslide hazard evaluation: a review of current techniques and their application in a multi-scale study, Central Italy. *Journal of Geomorphology, 31*, 181–216. Elsevier, London.

Jibson, W. R., Edwin, L. H., & John, A. M. (2000). A method for producing digital probabilistic seismic landslide hazard maps. *Engineering Geology, 58*, 271–289.

Kouli, M., Loupasakis, C., Soupios, P., & Vallianatos, F. (2010). Landslide Hazard Zonation in High risk area of Rethymno Prefecture, Crete Island, Grece, Nat Hazards 52, 599–621 Landslide Hazard Zonation Atlas of India, Building Materials and Technology Promotion Council & Centre for Disaster mitigation and management, Anna University, Chennai, India (2003).

Lee, S., & Choi, U. (2003). Development of GIS Based geological hazard information system and its application for landslide analysis in Korea. *Geoscience Journal, 7*, 243–252.

Lee, S., & Pradhan, B. (2006). Landslide hazard assessment at Cameron Highland Malaysia using frequency ratio and logistic regression models. *Geophy Res Abstracts*, 8: SRef-ID:1607-7962/gra/EGU06-A-03241.

Lee, S., Ryu, J. H., Won, J. S., & Park, H. J. (2004). Determination and Publication of the weights for landslide susceptibility mapping using an artificial neural network. *Engineering Geology, 71*, 289–302.

Lee, S., Choi, J., & Min, K. (2004). Probabilistic landslide hazard mapping using GIS and remote sensing data at Boun, Korea. *International Journal of Remote Sensing, 25*, 2037–2052.

Luzi, L., Pergalani, F., & Terlien, M. T. J. (2000). Slope vulnerability to earthquake at sub-regional scale, using probabilistic technique and geographic information systems. *Engineering Geology, 58*, 13–336.

Malczewski, J. (1999). *GIS and multi-criteria decision analysis* (1st ed.). NY: Wiley. 392p.

Mason, P. J., Rosenbaum, M. S., & Moore, J. McM. (1998). Digital image texture analysis for landslide hazard mapping, *Geohazards in Engineering Geology, Special Publications, Geological Society, London, 15*, 297–305.

Muthu, K., & Petrou, M. (2007). Landslide Hazard Mapping Using an Expert System and a GIS. *IEEE Transaction on Geoscience and Remote Sensing*, *45*(2).

Mwasi, B. (2001). Land use conflicts resolution in a fragile ecosystem using Multi Criteria Evalution (MCE) and a GIS based Decision Support System (DSS).

Nagarajan, R., Roy, A., Vinod Kumar, R., Mukherjee, A., & Khire, M. V. (2000). Landslide hazard susceptibility mapping based on terrain and climatic factors for tropical monsoon regions. *Bull Eng. Geol. Env.* 58.

Nie, H.F., Diao, S.J., Liu, J.X., & Huang, H. (2001). The application of Remote Sensing technique and AHP-fuzzy method in comprehensive analysis and assessment for regional stability of Chongqing City, China. Proceedings of the 22nd International Asian Conference on Remoye Sensing; November 5–9, 2001; University of Singapore, Singapore, 1:660–665.

Nithya, E. S., & Prasanna, R. P. (2010). An integrated approach with GIS and remote sensing technique for landslide zonation. *International Journal of Geomatics and Geosciences, 1*(1).

Pandey, A., Dabral, P. P., Chowdhary, V. M., & Yadav, N. K. (2008). Landslide hazard zonation using remote sensing and GIS: a case study of Dikrong river basin, Arunachal Pradesh, India. *Environmental Geology, 54*, 1517–1529.

Parise, M., & Jibson, W. R. (2000). A seismic landslide susceptibility rating of geologic units based on analysis of characteristics of landslides triggered by the 17 January, 1994 Northridge, California earthquake. *Engineering Geology, 58*, 251–270.

Pistocchi, A., Luzi, L., & Napolitano, P. (2002). The use of predictive modeling techniques for optimal exploitation of spatial databases: a case study in landslide hazard mapping with expert system-like methods. *Environmental Geology, 41*, 765–775.

Pradhan, B. (2010). Remote Sensing and GIS-based landslide hazard analysis and cross validation using multivariate logistic regression model on three test areas in Malaysia. *Advances in Space Research, 45*, 1244–1256.

Pradhan, B., & Lee, S. (2010a). Delineation of landslide hazard areas on Penang Island, Malaysia, by using frequency ratio, logistic regression, and artificial neural network models. *Environmental Earth Science, 60*, 1037–1054.

Pradhan, B., & Lee, S. (2010b). Landslide susceptibility assessment and factor effect analysis: backpropagation artificial neural networks and their comparison with frequency ratio and bivariate logistic regression modeling. *Environmental Modelling & Software, 25*, 747–759.

Pradhan, B., & Lee, S. (2010c). Regional landslide susceptibility analysis using back-propagation neural network model at Cameron Highland, Malaysia. *Landslides, 7*, 13–30.

Quinn, P., Beven, K., Chevallier, P., & Planchon, O. (1991). The prediction of hillslope flow paths for distributed gydrological modeling using digital terrain models. *Hydro Processes 5*, 59–79.

Rautelal, P., & Lakhera, R. C. (2000). Landslide Risk analysis between Giri and Tons Rivers in Himachal Himalaya (India). *International Journal of Applied Earth Observation and Geoinformation, 2*, 153–160

Rowbotham, D., & Dudycha, D. N. (1998). GIS Modelling of slope stability in Phewa Tal Watershed, Nepal. *Geomorphology, 26*, 151–170.

Saaty, T. L. (1977). A scaling method for priorities in hierarchical structures. *Journal of Mathematical Psychology, 15*, 234–281.

Saaty, T. L. (1980). *The analytical hierarchy process*. NY: McGraw Hill. 350p.

Saaty, T. L. (1990). *The analytical hierarchy process: Planning, priority setting, resource allocation* (1st ed.). Pittsburgh: RWS. 502p.

Saaty, T. L. (1994). *Fundamentals of decision making and priority theory with analytic hierarchy process* (1st ed.). Pittsburgh: RWS. 527p.

Saaty, T. L. (2000). Models, Methods, Concepts and Application of the Analytical Hierarchy Process, Boston:Kluwer Academic Publishers.

Saaty, T. L., & Vargas, L. G. (2001). *Models, methods, concepts and applications of the analytic hierarchy process* (1st ed.). Boston: Kluwer. 333p.

Saha, A. K., Gupta, R. P., & Arora, M. K. (2002). GIS based landslide hazard zonation in the Bhagirathi (Ganga) Valley, Himalayas. *International Journal of Remote Sensing, 23*, 357–369.

Sharifikia, M. (2007). "RS and GIS Application in Geo-hazard-A case study part of central Alborz-Iran"-Ph.D. Thesis submitted in Geology department, University of Delhi, India.

Sarkar, S., & Kanungo, D. P. (2004). An integrated approach for landslide susceptibility mapping using remote sensing and GIS. *Photogrammetric Engineering and Remote Sensing, 70*, 617–625.

Sharma, V. K. (2006). Landslide hazard zonation: an overview of emerging techniques. *Journal of Engineering Geology, XXXIII*, 73–80.

Soeters, R., & Westen, C. J. (1996). Slope instability recognition, analysis and zonation. In A. K. Turner and R. L. Schuster (Eds.), *Landslides: Investigation and Mitigation*. Transportation Research Board Special Report 247, 129–177.

Van Westen, C. J., Castellanos Abella, E., & Sekhar, L. K. (2008). Spatial data for landslide susceptibility, hazards and vulnerability assessment: an overview. *Engineering Geology, 102*, 112–131.

Varnes, D. J. (1984). Lanslide Hazard Zonation: a review of principles and practice. *UNESCO, Natural Hazard,* No. 3, pp 61.

Vijith, H., & Madhu, G. (2008). Estimating potential landslide sites of an upland sub-watershed in Western Ghat's of Kerala (India) through frequency ratio and GIS. *Environmental Geology, 55*, 1397–1405.

Yagi, H. (2003). Development of assessment method for landslide hazardness by Analytical Hierarchy Process (AHP). Abstract volume of the 42nd Annual Meeting of the Japan *Landsllide Society*, 209–212p.

Zhou, C. H., Lee, C. F., Li, J., & Xu, Z. W. (2002). On the spatial relationship between landslide and causative factors on Lantau Island, Hong Kong. *Geomorphology, 43*, 197–207.